

## Journal Pre-proofs

Green Synthesis and Properties of an Epoxy-Modified Oxidized Starch-Grafted Styrene-Acrylate Emulsion

Shaoxiang Li, Jiaping Wang, Wenjuan Qu, Jiaji Cheng, Yunna Lei, Dong Wang, Feng Zhang

PII: S0014-3057(19)31989-5

DOI: <https://doi.org/10.1016/j.eurpolymj.2019.109412>

Reference: EPJ 109412

To appear in: *European Polymer Journal*

Received Date: 6 October 2019

Revised Date: 25 November 2019

Accepted Date: 2 December 2019

Please cite this article as: Li, S., Wang, J., Qu, W., Cheng, J., Lei, Y., Wang, D., Zhang, F., Green Synthesis and Properties of an Epoxy-Modified Oxidized Starch-Grafted Styrene-Acrylate Emulsion, *European Polymer Journal* (2019), doi: <https://doi.org/10.1016/j.eurpolymj.2019.109412>

This is a PDF file of an article that has undergone enhancements after acceptance, such as the addition of a cover page and metadata, and formatting for readability, but it is not yet the definitive version of record. This version will undergo additional copyediting, typesetting and review before it is published in its final form, but we are providing this version to give early visibility of the article. Please note that, during the production process, errors may be discovered which could affect the content, and all legal disclaimers that apply to the journal pertain.

© 2019 Published by Elsevier Ltd.



## Green Synthesis and Properties of an Epoxy-Modified Oxidized Starch-Grafted Styrene-Acrylate Emulsion

Shaoliang Li<sup>a,b,c</sup>, Jiaping Wang<sup>a,b,c</sup>, Wenjuan Qu<sup>a,b,c,\*</sup>, Jiaji Cheng<sup>a,b,c</sup>, Yunna Lei<sup>a,b,c</sup>, Dong Wang<sup>a,b,c</sup>, Feng Zhang<sup>a,b</sup>

<sup>a</sup> College of Environment and Safety Engineering, Qingdao University of Science and Technology, Qingdao, 266042, P. R. China

<sup>b</sup> Shandong Engineering Research Center for Marine Environment Corrosion and Safety Protection, Qingdao University of Science and Technology, Qingdao, 266042, P. R. China

<sup>c</sup> Shandong Engineering Technology Research Center for Advanced Coating, Qingdao University of Science and Technology, Qingdao, 266042, P. R. China

\*Corresponding author, email [qwj\\_710@163.com](mailto:qwj_710@163.com)

### Abstract

An epoxy-modified oxidized starch-grafted styrene-acrylate (E-g-OS-P (BA-St)) emulsion was synthesized via soap-free core-shell emulsion polymerization without adding any solvent that could cause environmental problems. The emulsion exhibited excellent stability, chemical properties and mechanical performance. The synthesized emulsion was characterized by Fourier transform infrared spectroscopy (FTIR) and <sup>13</sup>C-NMR spectroscopy. Transmission electron microscopy (TEM) suggested that the OS-P (BA-St) latexes had certain umbrella structures and that the epoxy resin cross-linked a plurality of umbrella structures. Thermogravimetric analysis (TGA) and differential scanning calorimetry (DSC) showed that the thermal stability and glass transition temperature (T<sub>g</sub>) of the polymer became higher as the content of epoxy resin increased. Atomic force microscopy (AFM) was utilized to characterize the surface morphology of the films. The film with 10% epoxy resin (based on the mass of monomers) possessed superior tensile strength and elongation, exhibiting a nearly 100% increase in tensile strength relative to that of neat latexes without epoxy. Additionally, the mechanism of

polymerization and film formation of the E-g-OS-P (BA-St) emulsion were analysed.

**Keywords:** Emulsion; Epoxy resin; Oxidized starch; Properties.

## 1. Introduction

Poly(styrene-co-acrylate) is one of the most familiar emulsion copolymers. Its specific properties, including good film formation, gloss, transparency, and mechanical properties, make it significant in many fields [1-4]. Particles with core-shell morphology have some advantages over pure polymer particle and can be designed for versatile properties. Therefore, researchers have developed multiple approaches to improve poly(styrene-co-acrylate) emulsions. Tan synthesized a poly(styrene-co-butyl acrylate) emulsion via a structured core-shell particle design, finding that the polymer exhibited high cohesive and adhesive strength when the core-shell ratio was 1:1.5 [5]. Eren and coworkers developed novel core-shell-style styrene acrylic polymers to reduce the N-hydroxymethyl acrylamide (NMA) content and formaldehyde formation from pigment printing [6]. However, a series of shortcomings, such as poor water resistance, poor heat resistance, low pencil hardness, and high cost, still greatly limited the application of the materials [7]. In recent years, core-shell-style styrene acrylic polymers have been improved by changing the ratio between butyl acrylate (BA) and styrene (St) monomers or the order of the two monomers in the shell polymerization process [8-10], as well as by alternating the surfactant and initiator in the polymerization process [11, 12]. Additionally, core-shell-style styrene acrylic polymers can be modified by functional materials. Chen mixed PS-Ag conductive particles with particles of poly(styrene-co-butyl acrylate) and obtained large-scale anisotropic conductive films [13]. In addition, chemical modification of styrene-acrylic emulsions is a common method of improving their performance. By adding acrylonitrile to the shell material, acrylonitrile-styrene-acrylate (ASA) latexes were prepared to obtain a thicker latex shell structure, which improved the mechanical properties of the emulsion film [14]. A silane-modified styrene-acrylic emulsion improved the waterproof performance and softening coefficient of FGD gypsum products [3]. However, a relatively low level of corrosion protection, especially for

compositions without special protective ingredients, is the main drawback [15-17]. Coatings are a good barrier against the permeation of water, oxygen, and other corrosive species but can be quite weak due to various factors, such as residual hydrophilic components and a low cross-linking degree, which are often related to the use of a purely physical curing mechanism.

Starch is a carbohydrate obtained from plant photosynthesis and has the advantages of biocompatibility, biodegradability, low cost and no toxicity [18-20]. Starch has received extensive attention in the food [21], biomedical [22], wastewater treatment [23, 24], paper [25], and textile industries [26] because of its unique biological and adsorption properties. However, native starch has low shear stress resistance, low decomposition, high retrogradation, and syneresis properties. Moreover, its large molecular weight and condensation limit the application of native starch in many fields [27, 28]. Extensive work on starch modification has been implemented to overcome these inherent defects and achieve innovative starch applications; the techniques included physical processes [29-31] chemical modifications [32-35] enzymatic [36, 37] and biotechnological approaches [38] and combinations thereof. Some properties, including gelatinization temperature [39], thermal stability [40], rheological properties, paste clarity [41], and mechanical strength [42], can be improved via chemical modification. Starch oxidation is an important part of the chemical modification of starch. Researchers usually oxidize starch and apply the oxidized starch to other polymers. The introduction of grafted starch can improve the elasticity of PBA chains [43]. Meshram grafted St and MMA/BA onto starch molecules and observed a higher tensile strength and lower elongation at break when the material was used in cotton yarn [44]. Therefore, the synthesis of starch graft copolymers to combine the advantages of natural and synthetic polymers has aroused interest from many researchers. Gaborieau proved that the application properties of starch graft copolymers were better than those of common latex [45, 46]. Cheng succeeded in preparing oxidized starch-graft-poly-(styrene-butyl acrylate) and proved that the prepared polymer colloid had strong stability, fine particles and strong permeability [46-48]. Disappointingly, its adhesion and water resistance did not reach elevated

expectations.

In nature, epoxy resin is a kind of polymer that has advantages such as good thermal characteristics, excellent adhesion, and good chemical and corrosion resistance [49-51]. Deng and Djukic blended epoxy resin with a polymer to study the possible mechanism of their interfacial adhesion [51]. Zhang found that epoxy helped amine-containing benzoxazine-based homopolymers overcome the conversion limitation and promoted the curing rate [52]. Epoxy-modified styrene-acrylic emulsions have the dual properties of an epoxy resin and styrene-acrylic emulsion, where the epoxy resin is used as a cross-linking agent. Epoxy resin contains polar groups, including hydroxyl groups and epoxy groups, which easily form secondary bonds, hydrogen bonds and main valence bonds with many surface substances. Moreover, epoxy and hydroxyl groups can react with functional groups on other compounds (such as amino groups, hydroxyl groups and carboxyl groups) to form a network structure [53,54]. Thus, styrene-acrylic emulsions modified with epoxy resin possess strength, corrosion resistance and adhesion. Such emulsions have been widely applied to improve viscosity, mixture and coating properties [55, 56]. However, due to the high viscosity of epoxy resin, an excessive addition amount causes the polymer emulsion to gel. Additionally, organic solvents used as dispersion media cause residual organic solvent and environmental pollution.

In this work, the polymerization monomer participating in the reaction was used as a dispersion medium for the epoxy resin, avoiding environmental problems caused by volatilization of the organic solvent. E-g-OS-P (BA-St) latexes, which integrate the advantages of epoxy, oxidized starch and styrene-acrylate emulsions, were synthesized via soap-free core-shell emulsion polymerization. This approach has not been previously researched. The effect of the amount of epoxy resin on the properties of E-g-OS-P (BA-St) latex was studied. The obtained latexes are expected to have excellent chemical properties, thermal stability and mechanical properties. The introduced oxidized starch is biodegradable and ecofriendly. Oxidized starch can not only improve the dispersion stability of emulsions but also reduce the cost of emulsion production. Additionally, the mechanisms of polymerization and film formation were analysed,

which can provide a theoretical reference for coating applications.

## 2. Materials and methods

### 2.1. Materials

Oxidized starch was provided by Shangdong Jincheng Co., Ltd. Styrene (St, AR) and butyl acrylate (BA, AR) were purchased from Shanghai Chemical Reagent Co. and were purified by distillation under reduced pressure. Epoxy resin was supplied by Xinhua Resin Manufacturing, Shanghai Coatings Co. Hydrogen peroxide ( $\text{H}_2\text{O}_2$ , 30%) was obtained from Tianjin Damao Chemical Reagent Factory, China. Deionized water was prepared in our laboratory.

### 2.2. Preparation of oxidized starch

The corn starch (30g) and deionized water (120g) were weighed into the four-necked flask, which was placed with a stirrer and thermometer. Premixed at  $75^\circ\text{C}$  for 10 min, 0.12g  $\text{FeSO}_4$  was added. Then, 4.5g  $\text{H}_2\text{O}_2$  (30%) was slowly introduced dropwise. After the addition was completed, the oxidation reaction was conducted for 1 hour at temperature of  $70^\circ\text{C}$ .

### 2.3. Preparation of the E-g-OS-P (BA-St) latexes

After increasing the temperature to  $80^\circ\text{C}$ , the core monomer butyl acrylate (BA, 22.5g) and the initiator ( $\text{H}_2\text{O}_2$ , 2.625g) were added dropwise for 1.0 hours (the initiator droplet acceleration was expected to be slower than the monomer droplet acceleration). After a certain period of reaction, a mixture of epoxy resin dispersed evenly in styrene and initiator ( $\text{H}_2\text{O}_2$ , 2.625g) were added dropwise in the same manner. Based on the weight of the monomers, the epoxy resin content varied (0%, 2.5%, 5%, 10%, 15% and 20%), and the resulting materials were labelled E-0, E-1, E-2, E-3, E-4 and E-5, respectively. Specific amount of components was shown in Table 1. All of the reagents were kept for 1.5 hours after addition, and the E-g-OS-P (BA-St) emulsion was thus completed.

**Table 1**

**Formulations of E-g-OS-P (BA-St) latexes based on specific amount of components; E-0, E-1, E-2,**

E-3, E-4, E-5.

Material	E-0	E-1	E-2	E-3	E-4	E-5
Starch	30g	30g	30g	30g	30g	30g
H <sub>2</sub> O	120g	120g	120g	120g	120g	120g
FeSO <sub>4</sub>	0.12g	0.12g	0.12g	0.12g	0.12g	0.12g
H <sub>2</sub> O <sub>2</sub>	6.0g	6.0g	6.0g	6.0g	6.0g	6.0g
BA	22.5g	22.5g	22.5g	22.5g	22.5g	22.5g
St	22.5g	21.375g	20.25g	18g	15.75g	13.5g
Epoxy resin	0.0g	1.125g	2.25g	4.5g	6.75g	9g

#### 2.4. Film formation of E-g-OS-P (BA-St) latexes

The micro-latex was cast in a mould made of PTFE with a length of approximately 100 mm and a depth of approximately 1 mm. After bubbles were eliminated, the plate was placed at room temperature (25 °C) for 24 hours and then placed in an oven at 80 °C for 4 h. The mould was placed horizontally, forming a uniform-thickness film. After that, the film was carefully peeled from the mould and put into a desiccator with a valve bag.

### 3. Characterization

#### 3.1. Conversion and gel fraction

The conversion and gel fraction percentage were determined by a gravimetric technique.

A few drops of hydroquinone aqueous solution were added, and a certain mass ( $W_1$ ) of emulsion was weighed into a dry culture dish. The mass of the dry culture dish was labelled  $W_0$ . Afterwards, the sample was placed in an oven at 120 °C and dried to constant weight ( $W_2$ ).

The monomer conversion was calculated as follows [57-59]:

$$\delta = \frac{\frac{W_2 - W_0}{W_1} \times W_t - W_d}{W_a} \times 100\%$$

where  $W_1$  is the weight of the wet sample,  $W_2$  represents the weight of the dry sample,  $W_0$  is the weight of the culture dish,  $W_t$  is the total amount of reactants,  $W_d$  is the weight of non-volatiles in the initial formulation, and  $W_a$  represents the initial monomer weight.

The coagulum was obtained by filtration of the entire residue on the flask walls and mechanical stirrer. Then, the emulsion was filtered with a 200-mesh nylon gauze. After rinsing with deionized water, the residue and coagulum were placed in a watch glass and dried in an oven at 120 °C for 2 hours.

The formula for calculating the gel fraction is as follows:

$$\tau = \frac{M_3 - M_4}{M} \times 100\%$$

where  $M_3$  is the weight of the residue and coagulum,  $M_4$  is the watch glass weight, and  $M$  is the total weight of the emulsion.

### **3.2. Zeta potential**

Zeta potential ( $\zeta$ ) of the emulsions was determined by using a Particle Sizer and Zeta Potential Analyzer NanoBrook Omni (Brookhaven, USA). Emulsions were diluted (1:100) before test to avoid multiple scattering effects [60]. The data were calculated by the instrument using the Smoluchowski model and expressed in the unit of mV. All measurements were performed in triplicate, and measured within 2 hours after preparation. Four samples of each material were analysed and averaged.

### **3.3. Fourier transform infrared spectroscopy (FTIR)**

FTIR was performed in the wavenumber region between 4000 and 400  $\text{cm}^{-1}$  using the KBr pellet technique. The FTIR spectra were collected at a resolution of 4  $\text{cm}^{-1}$  and average of 32 scans using a Nicolet IS10 Thermo Scientific spectrophotometer.

### **3.4. $^{13}\text{C}$ -Nuclear magnetic resonance (NMR) spectroscopy**

The copolymer sequence distribution was measured with a Varian XL-400 spectrometer, which was operated at 100 MHz. Each sample was diluted to a concentration of 0.1 (g/mL) and characterized under the following conditions: width 20,000 Hz, acquisition time 0.4 s, flip angle 45°, pulse delay 1.6 s, and number of scans 512.  $\text{D}_2\text{O}$  was used as a locking agent for all nuclear magnetic resonance (NMR) spectra.

### **3.5. Transmission electron microscopy (TEM)**

The structural morphology of the latex particles was observed by transmission

electron microscopy (TEM) using a JEM-100 CX instrument (JEOL Co., Japan). The latexes were diluted with deionized water, diluted on a copper grid and dried in open air. Then, the samples were stained with phosphotungstic acid (PTA) solution (1.5%) before microscopic analysis [14].

### **3.6. Thermal properties**

Thermogravimetric analysis (TGA) was performed in a TGA/SDTA 851 thermobalance from Mettler Toledo, Inc. (Schwerzenbach, Switzerland). The heating program was set from 30 to 700 °C at a heating rate of 20 °C/min. The glass transition temperature was determined by differential scanning calorimetry (DSC) using a differential scanning calorimeter (Perkin Elmer, Pyris Diamond) calibrated with indium and zinc standards. Samples were cut from the dried films. For each measurement, a sample of  $8.0 \pm 0.2$  mg was heated from -50 °C to 150 °C with a heating rate of 10 °C/min under dry nitrogen atmosphere.

### **3.7. Atomic force microscope (AFM)**

The film surface morphology was measured by atomic force microscope in tapping mode, utilizing the AFM model JSPM-4210 (JEOL USA Inc., Peabody MA, USA) with cantilever strength constant of 30 N/m and frequency constant of 315 kHz. The AFM micrographs of the films over the scanning areas of  $10 \times 10 \mu\text{m}^2$  was calculated by the software WS-M 5.0 Develop 8.1.

### **3.8. Mechanical properties**

All samples (shape as shown in Fig. 1) were cut into strips ( $75 \times 4$  mm) using a dual-blade shear cutter (JDC Precision Cutter 10 in., Thwing-Albert Instrument Company, West Berlin, New Jersey, United States). The mechanical properties, including the tensile strength (TS) and elongation at break (Eb), were measured using a universal testing machine (LLOYD model LR5K) with a 300 mm/min speed according to the ASTM standard method D822-12 [61, 62]. Four samples of each material were analysed and averaged. Shape and size of the sample for mechanical properties was shown in Fig. 1.

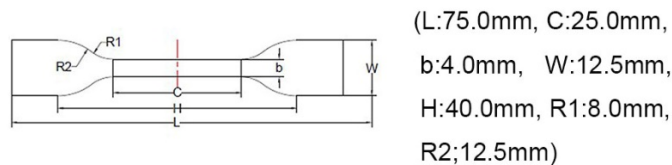


**Fig. 1. Shape and size of the sample for mechanical properties.**

## 4. Results and discussion

### 4.1. Physical–chemical characterization of the emulsions

Kan determined the storage stability of emulsions by adding electrolyte [63]. If latex is sensitive to the electrolyte, such as NaCl and Na<sub>2</sub>SO<sub>4</sub>, a certain amount of coagulum will appear. All the as-prepared latexes were resistant to NaCl and Na<sub>2</sub>SO<sub>4</sub>, even at their saturated concentrations. Moreover, there was no condensation when the latex was melted after being stored at -5 °C. No condensation occurred during storage for 6 months or during 1 hour of centrifugation at a speed of approximately 14,000 rpm, which implied that all latexes showed good storage stability and mechanical stability.

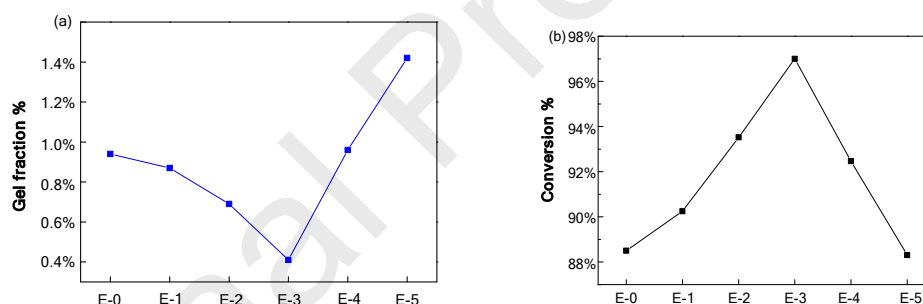


**Fig. 2. (a) Gel fraction of the as-prepared emulsion with different content of epoxy, E-0, E-1, E-2, E-3, E-4, E-5. (b) Monomer conversion of emulsion, E-0, E-1, E-2, E-3, E-4, E-5.**

As shown in Fig. 2, the emulsion without any epoxy resin added (E-0) had a monomer conversion of 88.45% and a gel content of 0.87%. The coagulum content decreased and then increased, and the emulsion monomer conversion tended to increase first and then decrease. The emulsion had the highest monomer conversion rate of 97% when the epoxy resin accounted for 10% of the monomer (E-3). However, E-3 had the lowest coagulum content of only 0.41%. This result may be because the molecular branches of the epoxy resin were dispersed between the molecular branches of the oxidized starch by stirring and dispersal; the spacing between starch molecules became large, and the probability of hydrogen bond formation between molecules was greatly

reduced. Therefore, it was possible to reduce the coagulum content of the emulsion within a certain range and improve the monomer conversion rate. However, the weakening of the interaction forces between the starch molecular chains increased with increased epoxy resin. In addition, the number of entanglement points between the epoxy resin and the starch molecules increased, intensifying the cross-linking reactions between the oxygen groups and the carboxyl groups on the branches of the starch molecules. A three-dimensional network structure was formed in which the medium was surrounded by the mesh and could not flow freely, thereby forming a gel in a semi-solid form.

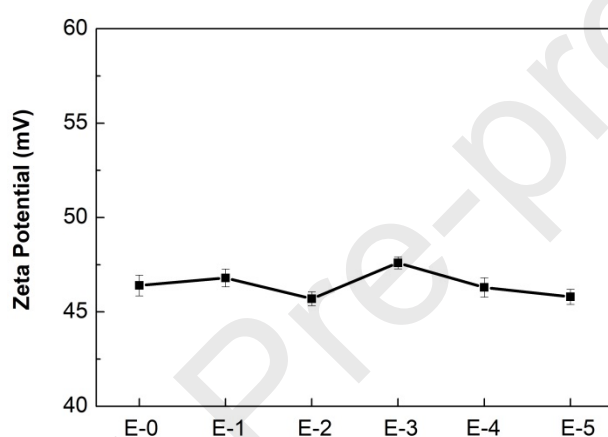


**Fig. 3. Zeta potential of emulsions, E-0, E-1, E-2, E-3, E-4, E-5.**

Zeta potential is carried out to determine the behavior of hydrocolloids at the oil-water interface, of which the vector surface charge provides indication of the long-term stability [64, 65]. Latexes emulsions with absolute value of zeta potential more than 30 mV are normally considered stable. Fig. 3 shows the emulsions have good stability that the zeta potential values were between 45.7 and 47.6mV. The zeta potential has little change, indicating the addition of epoxy resin didnt influence the stability of emulsions.

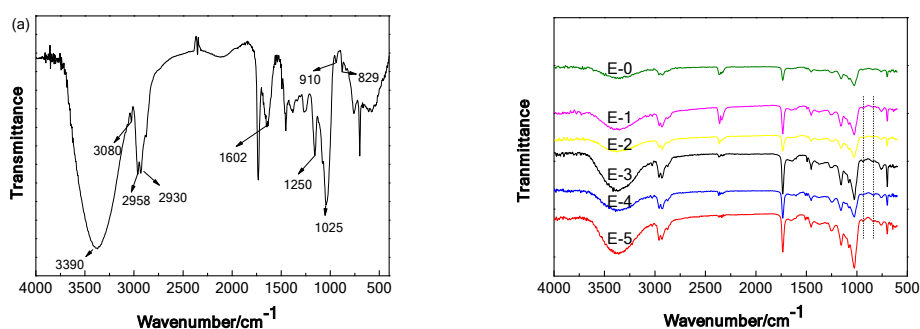


**Fig. 4. (a) Infrared spectra of E-g-OS-P (BA-St) emulsion. (b) Infrared spectra of emulsion, E-0, E-1, E-2, E-3, E-4, E-5.**

Fig. 4 (a) highlights the fingerprint zone of the main absorption peaks characterizing the E-g-OS-P (BA-St) latexes, which can be described as follows: The broad peak at approximately 3326–3648  $\text{cm}^{-1}$  corresponded to the telescopic vibration peak of –OH. The bands at 700-1100  $\text{cm}^{-1}$  could be assigned to the typical characteristic peaks of polysaccharides, which are a basic structural component of starch [23]. The appeared absorption peak at 2958 and 2930  $\text{cm}^{-1}$  is related to aliphatic C-H and –CH<sub>2</sub>. The peak at 3080  $\text{cm}^{-1}$  is attributed to aromatic ones. The strong peaks at approximately 1602  $\text{cm}^{-1}$  and 1025  $\text{cm}^{-1}$  were attributed to the aromatic C-C skeletal ring and the in-plane bending vibration of benzene ring C-H, respectively. The peak of acrylate components is their stretching vibration of carbonyl groups at 1720  $\text{cm}^{-1}$  [66]. The peaks detected near 1601  $\text{cm}^{-1}$  and 1250  $\text{cm}^{-1}$  were attributed to the stretching vibration of C-C and C-O-C bonds, respectively, which suggested that butyl acrylate and styrene participated in the starch graft copolymerization [43, 67]. The sharp peak at 1024  $\text{cm}^{-1}$  was attributed to the C-O stretching of C-O-C bonds in starch, which suggested  $\alpha$ -1,6 linkages [68, 69]. Fig. 4 (b) more intuitively shows the changes in the infrared spectra after the epoxy resin participated in the reaction. In Fig. 4 (b), the characteristic absorption peaks of epoxy resin near 829  $\text{cm}^{-1}$  and 910  $\text{cm}^{-1}$  indicated that epoxy resin participated in the polymerization of E-g-OS-P (BA-St) emulsion.

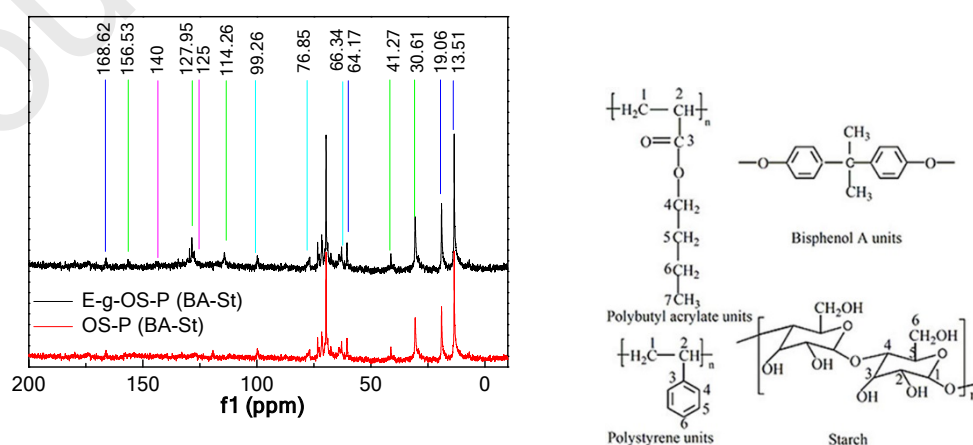


**Fig. 5. <sup>13</sup>C NMR spectrum of OS-P (BA-St) and E-g-OS-P (BA-St) emulsion.**

Fig. 5 shows the <sup>13</sup>C-NMR spectra for the E-g-OS-P (BA-St) latexes. The <sup>13</sup>C-

NMR spectrum had signals at 41.27, 168.62, 64.17, 30.61, 19.06, and 13.51 ppm, which have previously been assigned to C2, C3, C4, C5, C6, and C7 of polybutyl acrylate units [70, 71]. The C2-C5 carbons of polystyrene exhibited peaks at 125-130 ppm [72, 73].  $^{13}\text{C}$ -NMR demonstrated the character peak of C2-C6 of starch appeared at 60-75 ppm and the signal appeared at 99.7 ppm might be the characteristic peaks for C1 of the starch [74]. The chemical shifts at 114.26, 125, 140, and 156.53 ppm belonged to phenyl carbon in bisphenol A units. Characteristic shifts of P (BA-St) were also observed. These results demonstrated that the epoxy resin participated in emulsion polymerization.

#### 4.2. Polymerization mechanism

In general, the dominant reactions of starch oxidation are the oxidation of hydroxyl groups to carbonyl and carboxyl groups in the anhydroglucose units of starch and the decomposition of starch to low-molecular weight products with the catalyst  $\text{FeSO}_4$  and initiator  $\text{H}_2\text{O}_2$  [75, 76]. Detailed reaction mechanisms are given for carboxyl group formation at position C6 and carbonyl and carboxyl group formation by C2-C3 bond cleavage. It should be noted that the reaction schemes above do not represent complete stoichiometry.

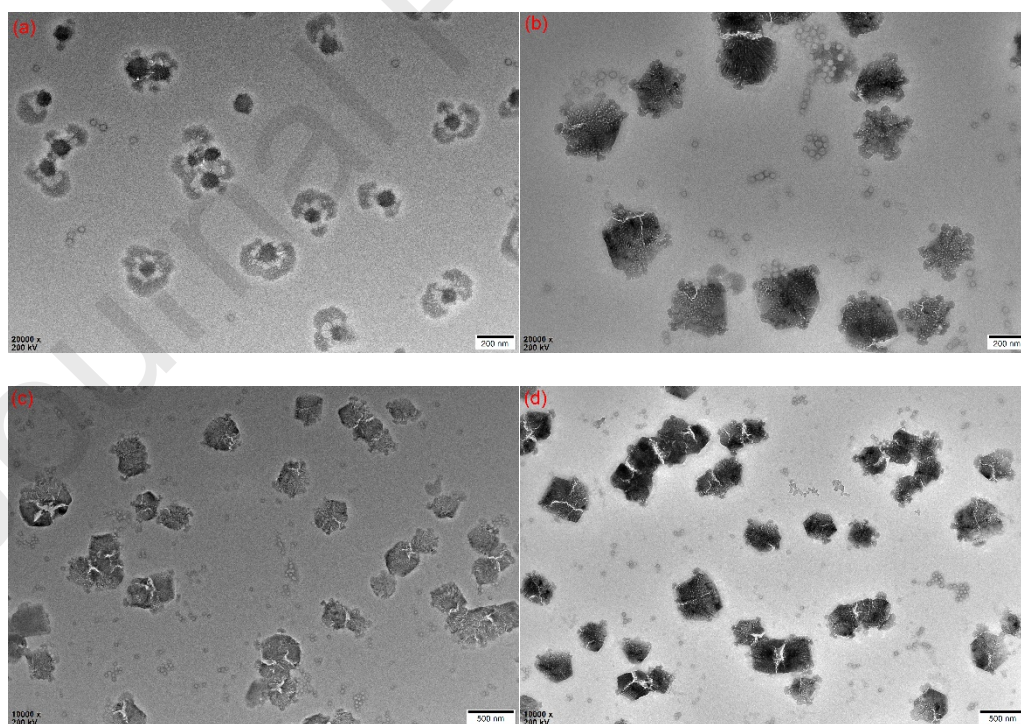
Reaction mechanisms of the whole process were displayed in Fig. 6. Free radicals were made from the ferrous ions in the polymerization medium according to the reaction mechanism shown in reaction (i). By abstracting hydrogen atoms from the pre-gelled starch molecules, the free radicals led to the formation of pre-gelled starch micro-radicals, as elucidated in reaction (ii). The pre-gelled starch radicals combined with the double bonds between the monomers of butyl acrylate and styrene, forming a growing chain between the starch and the monomer (iii). In the epoxy resin molecular chain, the H atoms on both the ortho carbons of ether bonds and tertiary carbons had relatively high activity and could be activated by the free radicals and become active points to initiate polymerization. Thus, graft copolymerization with the styrene and acrylate monomers was possible [56, 77]. The grafting reaction was as follows (iv). Fig. 7 shows simple schematic of the synthesis.



**Fig. 7. Schematic representation of the synthesis of OS-P (BA-St) particles and E-g-OS-P (BA-St) particles.**

### 4.3. TEM

Fig. 8 (a) displays a representative TEM micrograph of the OS-g-P (BA-St) latex particles. The P (BA-ST) latex distributed around the starch had a regular spherical structure. It could be concluded that the OS-g-P (BA-St) latex was synthesized and the P (BA-St) latex particles were randomly distributed on the edges of the oxidized starch granules, forming larger micro-emulsion particles. Fig. 8 (b)-(f) shows the colloidal particles formed by the participation of the epoxy resin in the emulsion polymerization. As the content of epoxy resin increased during the polymerization process, the latex particles became larger. Meanwhile, the H bonding was formed between oxygen of epoxy groups and hydroxy groups of starch. The epoxy resin promoted the crosslinking and formed larger micro-emulsion particles. Finally, at the same emulsion dilution concentration, the latex particles were connected into an overall network structure. Fig. 8 (f) granular morphology disappeared and exhibited as relative continuous film. It demonstrated that E-g-OS-P (BA-St) emulsion has better film forming properties.



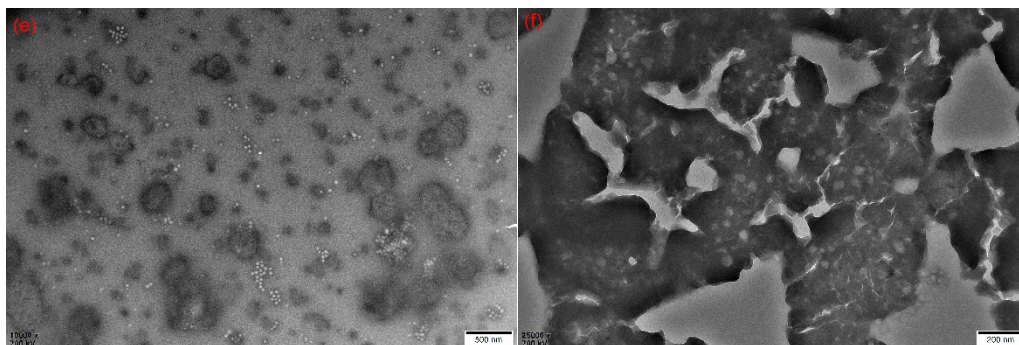


**Fig. 8. Representative TEM images of E-g-OS-P (BA-St) particles (a-f); E-0, E-1, E-2, E-3, E-4, E-5**

#### 5.4.4. Thermal properties and morphology of coating films

TGA can indicate the decomposition of polymers at various temperatures, which can be used to judge the thermal stability of different materials. Fig. 9 shows the thermal stability of OS-g-P (BA-St) latex and E-g-OS-P (BA-St) latex. OS-g-P (BA-St) latex decomposed in the range of 200–500 °C via two main processes. In the first process, the weight loss was 28.39% wt.%, which occurred at 200–320 °C and was attributed to the decomposition of oxidized starch. The DTGA image shows that the maximum decomposition rate occurred at 270 °C. The onset decomposition temperature of the second process was approximately 320 °C. 60.97 wt.% weight loss was detected from 320 °C to 500 °C, including a maximum decomposition rate at 380 °C. This process was related to the degradation of P (BA-St).

Many investigations have indicated that the char formed via cross-linking reactions enhances thermal stability [55, 78]. The E-g-OS-P (BA-St) latex had similar TG behaviour, with two different stages under the same conditions. The first weight loss was approximately 29.48 wt.% in the range from 220 to 350 °C. The second stage started at 350 °C and ended at 500 °C with a 58.59 wt.% weight loss. Both stages possessed higher temperature ranges of decomposition than those of the OS-g-P (BA-St) latex. The difference was that the decomposition temperature and weight loss in the first stage increased slightly with increased epoxy resin. The reason may be that the thermal decomposition of the one-component cured epoxy resin involved two stages. The first stage was in the range of 150–220 °C with a small decomposition, and the second stage was at 340–460 °C. Therefore, the starch and some of the epoxy resin were decomposed in the first-stage temperature range, resulting in an increase in the

decomposition temperature and weight loss in the first stage. Moreover, in the second stage, the E-g-OS-P (BA-St) latex had a higher decomposition temperature than the g-OS-P (BA-St) latex. The maximum amount of char residue increased by 135%, indicating that the E-g-OS-P (BA-St) latex possessed better thermal stability at high temperature. More details on the quality changes and residual char are shown in Table 2.

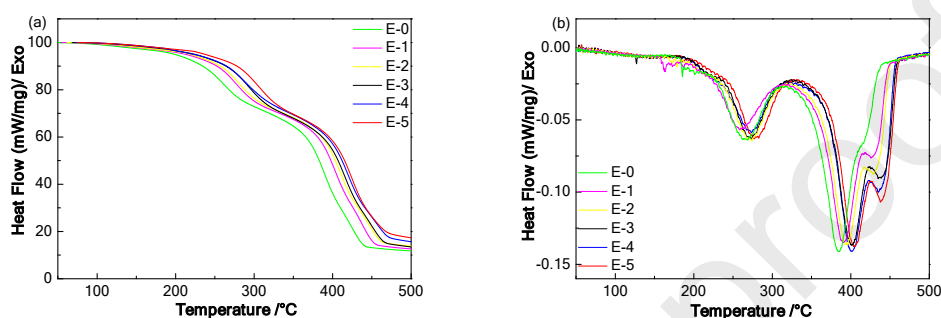


Fig. 9. (a) TGA thermogram of films; E-0, E-1, E-2, E-3, E-4, E-5. (b) DTG thermogram of films; E-0, E-1, E-2, E-3, E-4, E-5.

Table 2

Detailed quality changes, residual char residue and Tg of the films; E-0, E-1, E-2, E-3, E-4, E-5.

	E-0	E-1	E-2	E-3	E-4	E-5
weight loss in the first stage	28.39%	29.25%	29.48%	31.08%	29.97%	31.10%
weight loss in the second stage	60.97%	59.64%	58.59%	57.61%	57.08%	54.49%
char residue	10.64%	11.11%	11.93%	11.31%	12.95%	14.41%
Tg (°C)	70	75	78	81	86	95

DSC can be used to determine the distribution of polymer components. A single signal of  $dC_p/dT$  as a function of temperature is observed if the polymer components are well miscible [79]. Fig. 10 illustrates the DSC curves of the copolymers with different contents of epoxy resin. All the samples had only one glass transition because the monomer formed a stable polymer and the polymer did not show phase separation. The core-shell contents of different latex particles varied by a small amount, and the

glass transition temperature ( $T_g$ ) of the polymer ranged from 70 °C to 95 °C. As expected, the homogeneous copolymer copolymerized from oxidized starch, styrene and butyl acrylate showed only one  $T_g$  at 71 °C. This value was in reasonable agreement with the theoretical estimation of the  $T_g$  of a P (starch37.5- BA31.25-co-St31.25) copolymer according to the Fox-Flory equation ( $T_g$ , calculated = 64 °C). The E-5 copolymer had a glass transition temperature of 95 °C. The  $T_g$  of the polymer became higher as the epoxy resin content increased. This relation may be because the epoxy resin reacted with each component in a ring-opening reaction and penetrated the copolymer latex particles to form a three-dimensional network structure, which acted as a cross-linker. The specific explanation is as follows: the epoxy resin participated in the polymerization reaction in various forms. When dissolved in styrene, some of the epoxy resin participated as a polymeric monomer in the formation of the latex particle shell monomer, similar to styrene. Another part of the epoxy resin existed between the polymerized system of latex particles and oxidized starch due to its higher molecular weight. The epoxy resin caused cross-linking between polymer molecules, and the movement of the polymer segments was limited; thus, more energy was required to make these limited partial motions. Therefore, with increased epoxy resin in the polymer,  $T_g$  was increased.

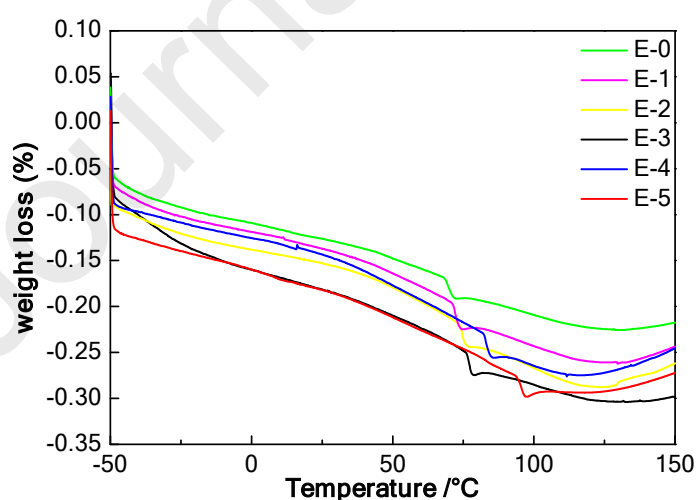
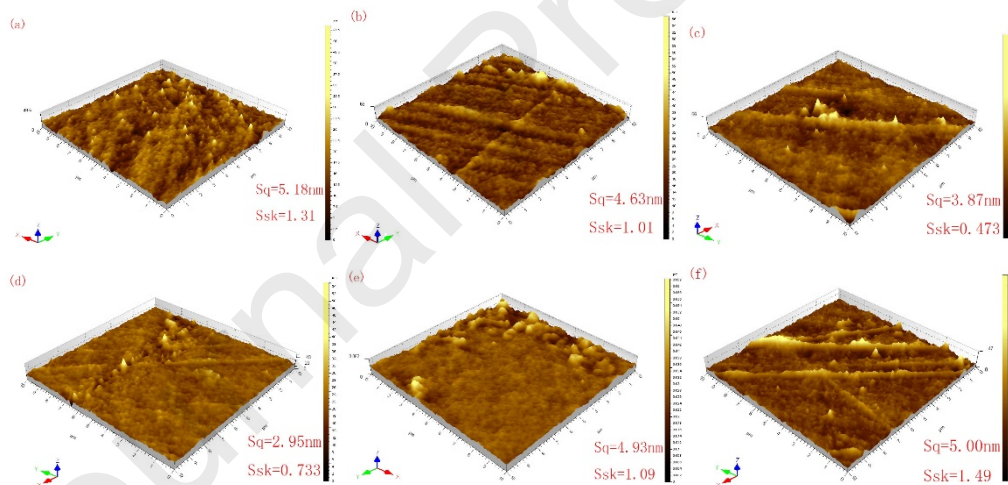


Fig. 10. DSC curves of the films; E-0, E-1, E-2, E-3, E-4, E-5.

Atomic force microscopy (AFM) was utilized to characterize the surface

morphology of the films [80]. Micromorphology of the film-air interface of the six latexes was observed by AFM as shown in Fig. 11. For all films, the value of Skewness (Ssk) were less than 3, suggesting that all the surfaces were flat enough [81]. The average roughness (Rq) of the films gradually decreased as epoxy increased within a certain range. It could be seen that as epoxy content was increased from 0 wt% to 10 wt%, Rq decreased from 5.18 nm to 2.95 nm. This may be because that as shown in Fig.11 (a), the starch particles were evenly distributed in the film. The addition of the epoxy resin enhanced the degree of crosslinking of the polymer particles, on the other hand, the epoxy resin acted as a kind of film former to participate in the formation of the polymer film, making the film flatter. However, as the content of the epoxy resin increased, phase separation occurred during the film formation, so that the formed film was not uniform and the roughness of the film turned to be larger.



**Fig.11 3D image profiles of emulsion films with the scanning areas of  $10 \times 10 \mu\text{m}^2$ : (a) E-0, Sq =5.18 nm, Ssk=1.31 (b) E-1, Rq =4.63 nm, Ssk=1.01 (c) E-2, Rq =3.87 nm, Ssk=0.473 (d) E-3, Rq =2.95 nm, Ssk=0.733 (e)E-4, Rq =4.93 nm Ssk=1.09 and (f) E-5, Rq =5.00 nm Ssk=1.49**

#### 4.5. Mechanical properties of the films

The mechanical properties of the films were determined by the ratio of soft to hard monomers in the latex particles and the content of starch [82]. All the films deformed in a brittle fashion. The tensile strength of the E-0 film was slightly lower than that of the styrene-acrylic emulsion after film formation [83], which was expected. This result may be because the starch had a large molecular weight and its addition would

inevitably reduce the fracture stress of the membrane and increase the brittleness of the polymer. With increasing epoxy resin content in the polymer, the tensile strength of the film gradually increased. The tensile strength of the E-5 film reached 4.1 MPa, which was 140% the film strength of E-0. However, the elongation at break of the film decreased as the epoxy resin content increased, to as low as 2%. Fig. 12 shows that the elongation at break of the E-4 film was drastically reduced. On the one hand, the highly cross-linked epoxy resin and starch formed a network that used the epoxy resin as a three-dimensional skeleton and used P (BA-St) as a matrix. Therefore, the tensile strength of the films was improved. In contrast, the addition of epoxy resin destroyed the continuity of the P (BA-St) matrix [84, 85], and excessive cross-linking decreased the mobility of short chains and made them likely stress concentration points under load. Consequently, the brittleness of the film became more obvious.

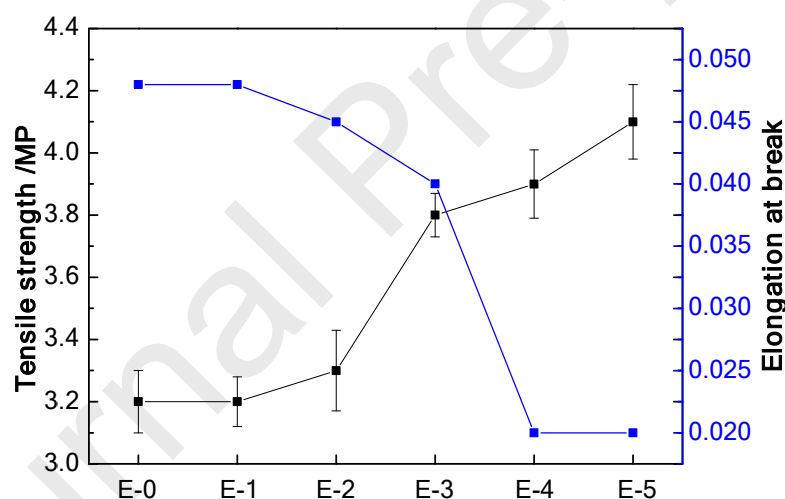


Fig. 12. Mechanical property of films; E-0, E-1, E-2, E-3, E-4, E-5.

#### 4.6. Mechanism of film formation

Steward et al. have studied the formation and properties of polymer latex films. They found that the properties of polymer films are not only affected by the properties of the polymer itself but also influenced by the polymer and film preparation processes [86, 87]. Latex deformation fusion and interdiffusion occur normally, forming a continuous transparent film, when an emulsion is formed at the minimum film formation temperature (MFFT). However, the polymer segments of the closely packed

latex particles cannot easily diffuse and fuse, and a continuous film cannot be formed, under fast water evaporation conditions [88]. Therefore, the emulsion was dried at room temperature for 24 hours and then placed in an oven at 80 °C for 4 hours.

A more reasonable model of emulsion film formation is proposed here. As shown in Fig.13, the process can be divided into three processes, including the evaporation process of water, the deformation process of particles, and the process of molecular diffusion, which is consistent with the film formation process of ordinary aqueous emulsions. There was no obvious time division among the processes [89, 90]. The first stage is the evaporation process of water. Due to the very fast evaporation rate of water, this stage was carried out at room temperature. Then, the latex particles were arranged in order and deformed under various forces, which is the second stage of film formation [91-93]. The epoxy resin cross-linked emulsion particles formed a polyhedral structure during the stacking process, and the core-shell structures of the particles also interacted and deformed, with blurred boundaries between particles. Although there was a certain free volume in the polymer system, the free volume was frozen, and the molecular segments were limited because the temperature was lower than the T<sub>g</sub> of the latex polymer. The third stage was carried out in an oven at 80 °C. As the particles were in contact with each other, the probability of surface contact increased. Segment movement across the molecular boundary occurred when the distance between the macromolecules of the latex particles was close enough and the particles had enough energy. The polystyrene in the hard-shell molecular segments in the core-shell structure interdiffused. At the same time, the polybutyl acrylate flexible core was uniformly dispersed in the hard shell to form a continuous phase [94-96]. The starch was uniformly distributed in the film, forming a sea-island structure. When the content of epoxy resin in the polymer was low, the epoxy resin could not form a continuous phase during the film formation process, affecting the mechanical properties of the film. When the amount of epoxy resin in the polymer was too high, the continuity of the P (BA-St) matrix was destroyed, and the toughness of the film was lowered.

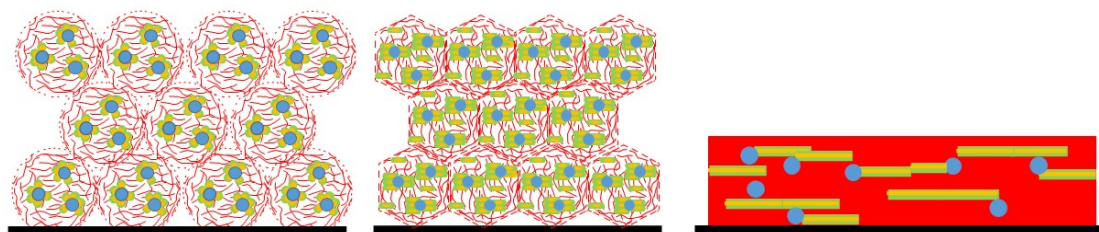


**Fig. 13. Schematic representation of the process of film formation.**

## 5. Conclusion

E-g-OS-P (BA-St) latexes were synthesized via soap-free core-shell emulsion polymerization without adding any solvent that could cause environmental problems. The addition of epoxy resin had an important effect on the morphology of E-g-OS-P (BA-St) latexes and the mechanical properties of the films. In addition, epoxy resin increased the thermal stability and T<sub>g</sub> of the films. When the epoxy resin content accounted for 10% of the total amount of the polymerized monomers, the emulsion exhibited good performance against low temperature, electrolyte and mechanical force. In addition, the formed film had excellent thermal stability. The film possessed a superior tensile strength of 4.5 MPa and elongation at break of 4%, representing a nearly 100% increase in tensile strength relative to that of neat latexes without epoxy. Moreover, this paper has proposed a possible model for film formation, which is very beneficial for further applications.

## Acknowledgements

This work was financially supported by the Natural Science Foundation of Shandong Province, China (No. ZR2016EMB20 and ZR2018MEE034), the National Natural Science Foundation of China (Grant No. 51806113) and the Postdoctoral Applied Research Program Fund of Qingdao (No. 2016204).

## References

- [1] T. Fardi, V. Pintus, E. Kampasakali, E. Pavlidou, M. Schreiner, G. Kyriacou, Analytical characterization of artist's paint systems based on emulsion polymers and synthetic organic pigments, *J. Anal. Appl. Pyrolysis* 135 (2018) 231-241.
- [2] S. Bowman, Q. Jiang, H. Memon, Y. Qiu, W. Liu, Y. Wei, Effects of styrene-acrylic sizing on the mechanical properties of carbon fiber thermoplastic towpreps and their composites, *Molecules* 23(3) (2018) 547.
- [3] Q. Wu, H. Ma, Q. Chen, B. Gu, S. Li, H. Zhu, Effect of silane modified styrene-acrylic emulsion on the waterproof properties of flue gas desulfurization gypsum, *Constr. Build. Mater.* 197 (2019) 506-512.

- [4] Y. Lu, Y. Xia, R.C. Larock, Surfactant-free core-shell hybrid latexes from soybean oil-based waterborne polyurethanes and poly (styrene-butyl acrylate), *Prog. Org. Coat.* 71(4) (2011) 336-342.
- [5] C. Tan, T. Tirri, C.-E. Wilen, The effect of core-shell particle morphology on adhesive properties of poly (styrene-co-butyl acrylate), *Int. J. Adhes. Adhes.* 66 (2016) 104-113.
- [6] M. Eren, G. Akbulut, S. Senler, B.K. Kayaoğlu, Synthesis of core-shell-type styrene acrylic latexes with low NMA content and their application in pigment printing pastes, *J. Coat. Technol. Res.* 15(1) (2018) 121-129.
- [7] R. Bai, T. Qiu, F. Han, L. He, X. Li, Preparation and characterization of emulsifier-free polyphenylsilsesquioxane-poly (styrene-butyl acrylate) hybrid particles, *Appl. Surf. Sci.* 282 (2013) 231-235.
- [8] H.-Y. Chen, H.-P. Shen, C.-H. Wu, W.-Y. Chiu, W.-C. Chen, H.-J. Tai, Core-shell composite latexes derived from PEDOT: PSS dispersion and the preparation of conductive, flexible and transparent films, *J. Mater. Chem. C* 1(34) (2013) 5351-5358.
- [9] A.E.I. Ahmed, A.I. Hussain, A.M. El-Masry, A. Saleh, Effect of Changing Mass Ratio of Styrene/Butyl Acrylate on the Behavior of Nano Organo-Silica in Poly (Styrene-Co-Butyl Acrylate) Emulsion Core-Shell, *ARN J. Eng. Appl. Sci* 10 (2015) 6127-6134.
- [10] J.-W. Kook, Y. Kim, K. Hwang, J. Kim, J.-Y. Lee, Synthesis of Poly (methyl methacrylate-co-butyl acrylate)/Perfluorosilyl Methacrylate Core-Shell Nanoparticles: Novel Approach for Optimization of Coating Process, *Polymers* 10(11) (2018) 1186.
- [11] F. Wang, Y. Luo, B.-G. Li, S. Zhu, Synthesis and redispersibility of poly (styrene-block-n-butyl acrylate) core-shell latexes by emulsion polymerization with RAFT agent-surfactant design, *Macromolecules (Washington, DC, U. S.)* 48(5) (2015) 1313-1319.
- [12] D. Jauregui, *Synthesis and Optimization of Emulsion Polymers*, (2016).
- [13] H.-Y. Chen, H.-P. Shen, H.-C. Wu, M.-S. Wang, C.-F. Lee, W.-Y. Chiu, W.-C. Chen, Synthesis of monodispersed polystyrene-silver core-shell particles and their application in the fabrication of stretchable large-scale anisotropic conductive films, *J. Mater. Chem. C* 3(14) (2015) 3318-3328.
- [14] S. Tolue, M.R. Moghbeli, S.M. Ghafelebashi, Preparation of ASA (acrylonitrile-styrene-acrylate) structural latexes via seeded emulsion polymerization, *Eur. Polym. J.* 45(3) (2009) 714-720.
- [15] D. Grigoriev, E. Shchukina, A. Tleuova, S. Aidarova, D. Shchukin, Core/shell emulsion micro- and nanocontainers for self-protecting water based coatings, *Surf. Coat. Technol.* 303 (2016) 299-309.
- [16] C.R. Hegedus, J.E. Sefko, C. Louis, W. Chaigneau, *Defoamers and wetting agents for waterborne alkyd coatings*, 2012, pp. 42-50.
- [17] O. Marchart, *Das unmögliche Objekt: eine postfundamentalistische Theorie der Gesellschaft*, Suhrkamp Verlag 2013.
- [18] S. Pérez, E. Bertoft, The molecular structures of starch components and their contribution to the architecture of starch granules: A comprehensive review, *Starch-Stärke* 62(8) (2010) 389-420.
- [19] C. Qiao, G. Chen, J. Zhang, J. Yao, Structure and rheological properties of cellulose nanocrystals suspension, *Food Hydrocolloids* 55 (2016) 19-25.
- [20] S. Mahmoudian, M.U. Wahit, A.F. Ismail, A.A. Yussuf, Preparation of regenerated

- cellulose/montmorillonite nanocomposite films via ionic liquids, *Carbohydr. Polym.* 88(4) (2012) 1251-1257.
- [21] P. Ambigaipalan, R. Hoover, E. Donner, Q. Liu, S. Jaiswal, R. Chibbar, K.K.M. Nantanga, K. Seetharaman, Structure of faba bean, black bean and pinto bean starches at different levels of granule organization and their physicochemical properties, *Food Res. Int.* 44(9) (2011) 2962-2974.
- [22] N. Masina, Y.E. Choonara, P. Kumar, L.C. du Toit, M. Govender, S. Indermun, V. Pillay, A review of the chemical modification techniques of starch, *Carbohydr. Polym.* 157 (2017) 1226-1236.
- [23] B. Xiang, W. Fan, X. Yi, Z. Wang, F. Gao, Y. Li, H. Gu, Dithiocarbamate-modified starch derivatives with high heavy metal adsorption performance, *Carbohydr. Polym.* 136 (2016) 30-37.
- [24] R. Cheng, S. Ou, Y. Li, B. Xiang, Kinetics and molecular mechanism of chromate uptake by dithiocarbamate functionalized starch, *J. Appl. Polym. Sci.* 124(4) (2012) 2930-2936.
- [25] S. Ni, H. Zhang, P.M. Godwin, H. Dai, H. Xiao, ZnO nanoparticles enhanced hydrophobicity for starch film and paper, *Mater. Lett.* 230 (2018) 207-210.
- [26] P. Zheng, T. Ma, X. Ma, Fabrication and properties of starch-grafted graphene nanosheet/plasticized-starch composites, *Ind. Eng. Chem. Res.* 52(39) (2013) 14201-14207.
- [27] M.M.S. Rivera, F.J.L.G. Suarez, M.G. Velazquez-Del Valle, F. Gutierrez-Meraz, L.A. Bello-Perez, Partial Characterization of banana starches oxidized by different levels of sodium hypochlorite, *Carbohydr. Polym.* 62(1) (2005) 50-56.
- [28] F. Haq, H. Yu, L. Wang, L. Teng, M. Haroon, R.U. Khan, S. Mehmood, R.S. Ullah, A. Khan, A. Nazir, Advances in chemical modifications of starches and their applications, *Carbohydr. Res.* 476 (2019) 12-35.
- [29] R.M. Astuti, N. Asiah, A. Setyowati, R. Fitriawati, Effect of physical modification on granule morphology, pasting behavior, and functional properties of arrowroot (*Marantha arundinacea* L) starch, *Food hydrocolloids* 81 (2018) 23-30.
- [30] K.N. Waliszewski, M.A. Aparicio, L.s.A. Bello, J.A. Monroy, Changes of banana starch by chemical and physical modification, *Carbohydr. Polym.* 52(3) (2003) 237-242.
- [31] S. Shabana, R. Prasansha, I. Kalinina, I. Potoroko, U. Bagale, S.H. Shirish, Ultrasound assisted acid hydrolyzed structure modification and loading of antioxidants on potato starch nanoparticles, *Ultrason. Sonochem.* 51 (2019) 444-450.
- [32] N.L. Vanier, S.L.M. El Halal, A.R.G. Dias, E. da Rosa Zavareze, Molecular structure, functionality and applications of oxidized starches: A review, *Food Chem.* 221 (2017) 1546-1559.
- [33] L.E. Mejía-Agüero, F. Galeno, O. Hernández-Hernández, J. Matehus, J. Tovar, Starch determination, amylose content and susceptibility to in vitro amylolysis in flours from the roots of 25 cassava varieties, *J Sci Food Agric.* 92(3) (2012) 673-678.
- [34] M. Haroon, L. Wang, H. Yu, N.M. Abbasi, M. Saleem, R.U. Khan, R.S. Ullah, Q. Chen, J. Wu, Chemical modification of starch and its application as an adsorbent material, *RSC Adv.* 6(82) (2016) 78264-78285.
- [35] U.B. Sandrine, V. Isabelle, M.T. Hoang, M. Chadi, Influence of chemical modification on hemp–starch concrete, *Constr. Build. Mater.* 81 (2015) 208-215.
- [36] Y. Benavent-Gil, C.M. Rosell, Morphological and physicochemical characterization of porous

- starches obtained from different botanical sources and amylolytic enzymes, *Int. J. Biol. Macromol.* 103 (2017) 587-595.
- [37] A. Rajan, J.D. Sudha, T.E. Abraham, Enzymatic modification of cassava starch by fungal lipase, *Ind. Crops Prod.* 27(1) (2008) 50-59.
- [38] M.N. Belgacem, A. Gandini, *Monomers, polymers and composites from renewable resources*, Elsevier 2011.
- [39] H. Winkler, W. Vorwerg, R. Rihm, Thermal and mechanical properties of fatty acid starch esters, *Carbohydr. Polym* 102 (2014) 941-949.
- [40] S. Pietrzyk, L. Juszczak, T. Fortuna, A. Ciemniowska, Effect of the oxidation level of corn starch on its acetylation and physicochemical and rheological properties, *J. Food Eng.* 120 (2014) 50-56.
- [41] O.V. López, M.A. García, N.E. Zaritzky, Film forming capacity of chemically modified corn starches, *Carbohydr. Polym* 73(4) (2008) 573-581.
- [42] M.M. Sánchez-Rivera, F.J.L. García-Suárez, M.V. Del Valle, F. Gutierrez-Meraz, L.A. Bello-Pérez, Partial characterization of banana starches oxidized by different levels of sodium hypochlorite, *Carbohydr. Polym* 62(1) (2005) 50-56.
- [43] S. Wang, J. Xu, Q. Wang, X. Fan, Y. Yu, P. Wang, Y. Zhang, J. Yuan, A. Cavaco-Paulo, Preparation and rheological properties of starch-g-poly (butyl acrylate) catalyzed by horseradish peroxidase, *Process Biochem. (Oxford, U. K.)* 59 (2017) 104-110.
- [44] M.W. Meshram, V.V. Patil, S.T. Mhaske, B.N. Thorat, Graft copolymers of starch and its application in textiles, *Carbohydr. Polym* 75(1) (2009) 71-78.
- [45] H. De Bruyn, E. Sprong, M. Gaborieau, G. David, J.A. Roper Iii, R.G. Gilbert, Starch-graft-copolymer latexes initiated and stabilized by ozonolyzed amylopectin, *J. Polym. Sci., Part A: Polym. Chem.* 44(20) (2006) 5832-5845.
- [46] M. Gaborieau, H. De Bruyn, S. Mange, P. Castignolles, A. Brockmeyer, R.G. Gilbert, Synthesis and characterization of synthetic polymer colloids colloidally stabilized by cationized starch oligomers, *J. Polym. Sci., Part A: Polym. Chem.* 47(7) (2009) 1836-1852.
- [47] S. Cheng, Y. Zhang, Y. Wu, Preparation and characterization of enzymatically degraded starch-g-poly (styrene-co-butyl acrylate) latex for paper coating, *Polym.-Plast. Technol. Eng.* 53(17) (2014) 1811-1816.
- [48] S. Cheng, Y. Zhao, Synthesis of eccentric core-shell particles by surfactant-free emulsion polymerization with enzymatically hydrolyzed starch as the stabilizer, *Colloid Polym. Sci.* 295(11) (2017) 2233-2241.
- [49] F.-L. Jin, X. Li, S.-J. Park, Synthesis and application of epoxy resins: A review, *J. Ind. Eng. Chem. (Amsterdam, Neth.)* 29 (2015) 1-11.
- [50] M. Bulut, Mechanical characterization of Basalt/epoxy composite laminates containing graphene nanopellets, *Composites Part B: Engineering* 122 (2017) 71-78 %@ 1359-8368.
- [51] S. Deng, L. Djukic, R. Paton, L. Ye, Thermoplastic-epoxy interactions and their potential applications in joining composite structures-A review, *Compos Part A Appl S* 68 (2015) 121-132.
- [52] L. Zhang, M. Wang, J. Wu, Study on an amine-containing benzoxazine: Homo-and copolymerization with epoxy resin, *Express Polym. Lett.* 10(7) (2016) 617.
- [53] E. Yarahmadi, K. Didehban, M.G. Sari, M.R. Saeb, M. Shabaniyan, F. Aryanasab, P. Zarrintaj, S.M.R. Paran, M. Mozafari, M.J.P.i.O.C. Rallini, Development and curing potential of

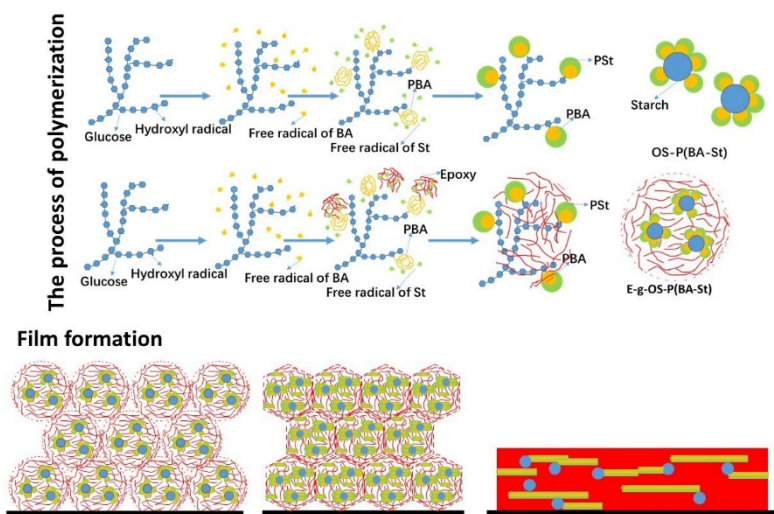
- epoxy/starch-functionalized graphene oxide nanocomposite coatings, *Prog. Org. Coat.* 194-202.
- [54] Keyvan Rad J, Mahdavian AR (2016) Preparation of fast photoresponsive cellulose and kinetic study of photoisomerization. *J Phys Chem C* 120 (2016) 9985–9991.
- [55] S. Torres-Giner, N. Montanes, T. Boronat, L. Quiles-Carrillo, R. Balart, Melt grafting of sepiolite nanoclay onto poly (3-hydroxybutyrate-co-4-hydroxybutyrate) by reactive extrusion with multi-functional epoxy-based styrene-acrylic oligomer, *Eur. Polym. J.* 84 (2016) 693-707.
- [56] G. Pan, L. Wu, Z. Zhang, D. Li, Synthesis and characterization of epoxy-acrylate composite latex, *J. Appl. Polym. Sci.* 83(8) (2002) 1736-1743.
- [57] D.G. Yu, J.H. An, J.Y. Bae, Y.E. Lee, S.D. Ahn, S.Y. Kang, K.S. Suh, Preparation and characterization of titanium dioxide core/polymer shell hybrid composite particles prepared by emulsion polymerization, *J. Appl. Polym. Sci.* 92(5) (2004) 2970-2975.
- [58] A. Romo-Urbe, J.A. Arcos-Casarrubias, A. Reyes-Mayer, R. Guardian-Tapia, Acrylate hybrid nanocomposite coatings based on SiO<sub>2</sub> nanoparticles. In-situ semi-batch emulsion polymerization, *Eur. Polym. J* 76 (2016) 170-187.
- [59] M. Sanei, S. Torabi, J.K. Rad, H. Salehi-Mobarakeh, A.R.J.M.C. Mahdavian, Physics, A thermo-kinetic study on acrylic copolymer nanocomposite particles containing GMA-modified nanosilica prepared via miniemulsion polymerization, *Mater. Chem. Phys.* 240 (2020) 122-126.
- [60] R. Sukhotu, S. Guo, J. Xing, Q. Hu, R. Wang, X. Shi, K. Nishinari, Y. Fang, S.J.L.-F.S. Guo, Technology, Changes in physiochemical properties and stability of peanut oil body emulsions by applying gum arabic, *LWT--Food Sci. Technol.* 68 (2016) 432-438.
- [61] D.J.A.b.o.A.s. ASTM, Standard test method for tensile properties of thin plastic sheeting, 8 (1995) 182-190.
- [62] J.D. Rusmirović, M.P. Rančić, V.B. Pavlović, V.M. Rakić, S. Stevanović, J. Djonlagić, A.D.J.M.M. Marinković, Engineering, Cross - Linkable Modified Nanocellulose/Polyester Resin-Based Composites: Effect of Unsaturated Fatty Acid Nanocellulose Modification on Material Performances, *Macromol. Mater. Eng.* 303(8) (2018) 1700648.
- [63] C.Y. Kan, D.S. Liu, X.Z. Kong, X.L. Zhu, Study on the preparation and properties of styrene-butyl acrylate-silicone copolymer latices, *J. Appl. Polym. Sci.* 82(13) (2001) 3194-3200.
- [64] P. Shao, H. Ma, J. Zhu, Q.J.F.H. Qiu, Impact of ionic strength on physicochemical stability of o/w emulsions stabilized by *Ulva fasciata* polysaccharide, *Food Hydrocolloids* 69 (2017) 202-209.
- [65] X. Yan, Y. Ji, T.J.P.i.O.C. He, Synthesis of fiber crosslinking cationic latex and its effect on surface properties of paper, *Prog. Org. Coat.* 76(1) (2013) 11-16.
- [66] J. Keyvan Rad, A.R. Mahdavian, S. Khoei, S.J.A.a.m. Shirvalilou, interfaces, Enhanced photogeneration of reactive oxygen species and targeted photothermal therapy of C6 glioma brain cancer cells by folate-conjugated gold-photoactive polymer nanoparticles, *ACS Appl. Mater. Interfaces* 10(23) (2018) 19483-19493.
- [67] L.G. Ecco, S. Rossi, M. Fedel, F. Deflorian, Color variation of electrophoretic styrene-acrylic paints under field and accelerated ultraviolet exposure, *Mater. Design* 116 (2017) 554-564.
- [68] Z. Zhang, P. Chen, X. Du, Z. Xue, S. Chen, B. Yang, Effects of amylose content on property and microstructure of starch-graft-sodium acrylate copolymers, *Carbohydr. Polym* 102 (2014) 453-459.

- [69] M. Miao, R. Li, C. Huang, B. Jiang, T. Zhang, Impact of  $\beta$ -amylase degradation on properties of sugary maize soluble starch particles, *Food Chem.* 177 (2015) 1-7.
- [70] K. Katsuraya, K. Hatanaka, K. Matsuzaki, M. Minagawa, Assignment of finely resolved  $^{13}\text{C}$  NMR spectra of polyacrylonitrile, *Polymer* 42(14) (2001) 6323-6326.
- [71] Y. Iizuka, Y. Yamamoto, S. Kawahara, Latex-state  $^{13}\text{C}$ -NMR spectroscopy for poly (butyl acrylate), *Colloid Polym. Sci.* 297(1) (2019) 133-139.
- [72] M. Kopeć, R. Yuan, E. Gottlieb, C.M.R. Abreu, Y. Song, Z. Wang, J.F.J. Coelho, K. Matyjaszewski, T. Kowalewski, Polyacrylonitrile-b-poly (butyl acrylate) block copolymers as precursors to mesoporous nitrogen-doped carbons: synthesis and nanostructure, *Macromolecules* (Washington, DC, U. S.) 50(7) (2017) 2759-2767.
- [73] S. Wang, G.W. Poehlein, Investigation of the sequence distribution of bulk and emulsion styrene-acrylic acid copolymers by  $^1\text{H}$ -and  $^{13}\text{C}$ -NMR, *J. Appl. Polym. Sci.* 49(6) (1993) 991-1001.
- [74] Y. Li, Y. Tan, K. Xu, C. Lu, P. Wang, A biodegradable starch hydrogel synthesized via thiol-ene click chemistry, *Polym. Degrad. Stab.* 137 (2017) 75-82.
- [75] P. Tolvanen, A. Sorokin, P.i. Mäki-Arvela, D.Y. Murzin, T. Salmi, Oxidation of starch by  $\text{H}_2\text{O}_2$  in the presence of iron tetrasulfophthalocyanine catalyst: The effect of catalyst concentration, pH, solid-liquid ratio, and origin of starch, *Ind. Eng. Chem. Res.* 52(27) (2013) 9351-9358.
- [76] P. Tolvanen, A. Sorokin, P.i. Mäki-Arvela, S. Leveneur, D.Y. Murzin, T. Salmi, Batch and semibatch partial oxidation of starch by hydrogen peroxide in the presence of an iron tetrasulfophthalocyanine catalyst: The effect of ultrasound and the catalyst addition policy, *Ind. Eng. Chem. Res.* 50(2) (2010) 749-757.
- [77] J.T. Woo, V. Ting, J. Evans, C. Ortiz, G. Carlson, R. Marcinko, Water Dispersible Epoxy-g-Acrylic Copolymer for Container Coating, *ACS Symp. Ser.* 221 (1983) 283-300.
- [78] S.S. Nagane, S. Verma, B.V. Tawade, P.S. Sane, S.A. Dhanmane, P.P. Wadgaonkar, Aromatic polyesters containing pendant azido groups: Synthesis, characterization, chemical modification and thermal cross-linking, *Eur. Polym. J* 116 (2019) 180-189.
- [79] M. Gosecka, M. Gosecki, Characterization methods of polymer core-shell particles, *Colloid Polym. Sci.* 293(10) (2015) 2719-2740.
- [80] W. Tang, Z. Ye, Y. Chen, G.J.J.o.F.C. Lin, Synthesis and characterization of poly(fluorinated styrene-acrylate)/silica nanocomposites, 186 (2016) 52-59.
- [81] A.K. Bajpai, R. Bhatt, R.J.M. Katare, Atomic force microscopy enabled roughness analysis of nanostructured poly (diaminonaphthalene) doped poly (vinyl alcohol) conducting polymer thin films, 90 (2016) 12-17.
- [82] Z. Zhong, Q. Yu, H. Yao, W. Wu, W. Feng, L. Yu, Z. Xu, Study of the styrene-acrylic emulsion modified by hydroxyl-phosphate ester and its stoving varnish, *Prog. Org. Coat.* 76(5) (2013) 858-862.
- [83] J. Machotová, J. Šňupárek, L. Prokůpek, T. Rychlý, P. Vlasák, Effect of functionalised core-shell microgels prepared by emulsion polymerisation on acrylic coatings properties, *Prog. Org. Coat.* 63(2) (2008) 175-181.
- [84] S. George, R. Joseph, S. Thomas, K.T. Varughese, Blends of isotactic polypropylene and nitrile

- rubber: morphology, mechanical properties and compatibilization, *Polymer* 36(23) (1995) 4405-4416.
- [85] B. Meng, J. Deng, Q. Liu, Z. Wu, W. Yang, Transparent and ductile poly (lactic acid)/poly (butyl acrylate)(PBA) blends: Structure and properties, *Eur. Polym. J* 48(1) (2012) 127-135.
- [86] P.A. Steward, J. Hearn, M.C. Wilkinson, An overview of polymer latex film formation and properties, *Adv. Colloid Interface Sci.* 86(3) (2000) 195-267.
- [87] S.S. Umare, B.H. Shambharkar, R.S. Ningthoujam, Synthesis and characterization of polyaniline-Fe<sub>3</sub>O<sub>4</sub> nanocomposite: Electrical conductivity, magnetic, electrochemical studies, *Synth. Met.* 160(17-18) (2010) 1815-1821.
- [88] J.L. Keddie, Film formation of latex, *Mater. Sci. Eng., R: Reports* 21(3) (1997) 101-170.
- [89] I. de Fa Mariz, I.S. Millichamp, C. José, J.R. Leiza, High performance water-borne paints with high volume solids based on bimodal latexes, *Prog. Org. Coat.* 68(3) (2010) 225-233.
- [90] L.A. Felton, Mechanisms of polymeric film formation, *Int. J. Pharm. (Amsterdam, Neth.)* 457(2) (2013) 423-427.
- [91] Y. Ma, H.T. Davis, L.E. Scriven, Microstructure development in drying latex coatings, *Prog. Org. Coat.* 52(1) (2005) 46-62.
- [92] M. Visschers, J. Laven, R. van der Linde, Film formation from latex dispersions, *J. Coat. Technol. Res.* 73(916) (2001) 49-55.
- [93] J. Keddie, A.F. Routh, *Fundamentals of latex film formation: processes and properties*, Springer Science & Business Media 2010.
- [94] W.F. Schroeder, Y. Liu, J.P. Tomba, M. Soleimani, W. Lau, M.A. Winnik, Effect of a coalescing aid on the earliest stages of polymer diffusion in poly (butyl acrylate-co-methyl methacrylate) latex films, *Polymer* 52(18) (2011) 3984-3993.
- [95] E. Arda, Ö. Pekcan, Time and temperature dependence of void closure, healing and interdiffusion during latex film formation, *Polymer* 42(17) (2001) 7419-7428.
- [96] S. Kara, Ö. Pekcan, A. Sarac, E. Arda, Film formation stages for poly (vinyl acetate) latex particles: a photon transmission study, *Colloid Polym. Sci.* 284(10) (2006) 1097-1105.

**Highlights**

1. Epoxy-modified oxidized starch grafted styrene-acrylate emulsion (E-g-OS-P(BA-St)) which integrate the advantages of epoxy, oxidized starch and styrene-acrylate emulsion were synthesized via soap-free core-shell emulsion polymerization.
2. The monomers participating in emulsion polymerization were used as dispersion medium for the epoxy resin, avoiding environmental problems caused by volatilization of the organic solvent.
3. The epoxy resin plays an important effect on properties of E-g-OS-P(BA-St) emulsion. The mechanism of polymerization and film formation were analyzed, which can provide theory reference for coating application.



Journal Pre-proofs

**Shaoliang Li:** Conceptualization, Writing- Reviewing and Editing,  
Supervision

**Jiaping Wang:** Software, Writing-Original draft preparation, Formal  
analysis

**Wenjuan Qu :** Conceptualization, Methodology, Writing-Original draft  
preparation, Writing- Reviewing and Editing, Supervision, Funding  
acquisition

**Jiaji Cheng:** Investigation, Writing- Reviewing and Editing, Funding  
acquisition

**Yunna Lei :** Software

**Dong Wang :** Methodology, Formal analysis

**Feng Zhang :** Investigation, Funding acquisition

**Conflicts of interest**

We declare that we have no financial and personal relationships with other people or organizations that can inappropriately influence this work, there is no conflicts of interest to this work.

Journal Pre-proofs